ISSN 1070-3284, Russian Journal of Coordination Chemistry, 2019, Vol. 45, No. 9, pp. 626–636. © Pleiades Publishing, Ltd., 2019.
Russian Text © The Author(s), 2019, published in Koordinatsionnaya Khimiya, 2019, Vol. 45, No. 9, pp. 527–538.

Tin(II) Complexes Based on *N*-Alkyl-Substituted *o*-Amidophenolate Ligands: Acid–Base and Redox Transformations

A. V. Piskunov[a], *, K. V. Tsys[a], M. G. Chegerev[b], and A. V. Cherkasov[a]

[a] *Razuvaev Institute of Organometallic Chemistry, Russian Academy of Sciences, Nizhny Novgorod, Russia*
[b] *Research Institute of Physical and Organic Chemistry, Southern Federal University, Rostov-on-Don, Russia*
**e-mail: pial@iomc.ras.ru*

Received March 27, 2019; revised April 24, 2019; accepted April 25, 2019

Abstract—New stannylene ^{Ad}APSn (**I**) based on 4,6-di-*tert*-butyl-*N*-adamantyl-*o*-aminophenol is synthesized and structurally characterized. Stannylene **I** in the crystalline state forms infinite chains due to intermolecular donor–acceptor Sn–N and metallophilic Sn···Sn interactions. The reactivities of compound **I** and earlier synthesized $^{t\text{-Bu}}$APSn (**II**) are studied using their redox and acid–base reactions. Stannylenes **I** and **II** are inserted at the S–S bond of tetramethylthiuram disulfide to form the corresponding tin(IV) dithiocarbamate complexes. The reactions with soft one-electron oxidants involve the redox-active *o*-amidophenolate ligand and generate labile paramagnetic stannylenes studied by EPR spectroscopy. The presence of a lone electron pair at the low-valence tin atom is a reason for its basic properties, which is demonstrated for the reaction of compound **I** with nanocarbonyl iron. The structures of selected synthesized compounds are determined by X-ray diffraction analysis (CIF files CCDC nos. 1905419–1905421).

Keywords: tin, carbene analogs, one-electron oxidation, X-ray diffraction analysis, electron paramagnetic resonance

DOI: 10.1134/S1070328419090069

INTRODUCTION

Coordination and organometallic compounds containing redox-active ligands are among promising points of the development of modern chemistry and find use in the whole series of investigation areas, such as fundamental problems of the chemical bond theory, catalytic transformations of organic substrates and small molecules, molecular magnetism, and many others [1–8]. Studies of compounds of nontransition metals in low oxidation states with unique chemical properties became another intensively developed trend of coordination chemistry [9–13]. Among them, serious attention is given to divalent derivatives of 14 Group elements, so-called heavy analogs of carbenes. A large information body about the synthesis and chemical properties of stable germylenes, stannylenes, and plumbylenes has been accumulated in the literature to the present time [14–20]. The introduction of redox-active ligands (*o*-quinones [21, 22], *o*-iminoquinones [22–27], and α-diimines [28–34]) into the composition of heavy carbene analogs made it possible to formulate the new branch of the development of the chemistry of low-valence metal derivatives for which the ranges of redox transformation are substantially extended. Now it is possible to synthesize principally new paramagnetic carbene analogs [33, 34] and also to use them as donor ligands in the design of coordination compounds of transition metals [35]. This work is devoted to the synthesis and study of the chemical properties of stannylenes: the tin(II) complexes based on the redox-active 4,6-di-*tert*-butyl-*N*-(alkyl)-*o*-aminophenolate ligands.

EXPERIMENTAL

All procedures on the synthesis and studies of chemical transformations of the tin complexes were carried out in the absence of air oxygen and moisture. The solvents used in the work were purified and dehydrated according to published recommendations [36]. Tetramethylthiuram disulfide (TMTDS) and mercury(II) halides were commercial reagents. 2-Ethoxy-3,6-di-*tert*-butylphenoxyl radical [37], $Fe_2(CO)_9$ [38], $Sn(N(SiMe_3)_2)_2$ [39], and $^{t\text{-Bu}}$APSn complex (**II**) [26] were synthesized according to known procedures. 4,6-Di-*tert*-butyl-*N*-(adamantyl)-*o*-aminophenol was synthesized by the reaction of 3,5-di-*tert*-butylpyrocatechol with 1-aminoadamantane [40, 41] using the modified procedure described earlier [42].

Synthesis of complex ^{Ad}APSn (I). $Sn(N(SiMe_3)_2)_2$ (0.444 g, 1 mmol) in Et_2O (20 mL) was added to a solution of 4,6-di-*tert*-butyl-*N*-(adamantyl)-*o*-aminophenol (1 mmol) in the same solvent (10 mL). The reaction mixture was stirred at room temperature

for 3 h. After the end of the reaction, the solvent was removed under reduced pressure. The yield of complex **I** as a diamagnetic crystalline yellow-orange powder was 0.38 g (80%).

For $C_{48}H_{70}N_2O_2Sn_2$		
Anal. calcd., %	C, 61.04	H, 7.47
Found, %	C, 61.12	H, 7.52

^{1}H NMR (C_6D_6, 20°C), δ, ppm: 7.23 (d, 1H, H_{AP}, J_{H-H} = 2.3 Hz); 6.83 (d, 1H, H_{AP}, J_{H-H} = 2.3 Hz); 1.88 (s, 9H, (*t*-Bu)); 1.83 (s, 3H, –CH–); 1.54 (s, 6H, $-CH_2-$); 1.45 (s, 6H, $-CH_2-$); 1.35 (s, 9H, (*t*-Bu)). ^{13}C NMR (C_6D_6, 20°C), δ, ppm: 138.1, 137.6 (C–(*t*-Bu)); 135.0 (C–O); 125.5 (C–N); 121.0–104.1 (C_{aryl}); 57.3 (N–C_{Ad}); 41.8, 36.0 (CH_{2Ad}); 32.0–31.1 (C_{quater}); 30.3 (CH_3(*t*-Bu)); 29.7 (CH_{Ad}). ^{119}Sn NMR (C_6D_6, 20°C), δ, ppm: –295.2.

IR (ν, cm^{-1}): 1583 w, 1554 w, 1533 s, 1409 w, 1395 m, 1323 w, 1304 w, 1270 m, 1248 m, 1239 m, 1213 w, 1183 w, 1157 m, 1136 w, 1115 w, 1096 m, 1052 w, 1026 w, 1005 m, 972 s, 944 w, 916 w, 902 m, 865 w, 851 m, 828 m, 806 w, 757 m, 732 s, 694 m, 652 m, 641 w, 615 w, 568 m, 542 w, 528 m, 507 m, 465 m.

Synthesis of complexes III and IV. A solution of TMTDS (1 mmol) in hexane (10 mL) was poured to a yellow solution of complex **I** or **II** (1 mmol) in CH_2Cl_2 (20 mL). The color of the reaction mixture instantly changed to red-violet. The reaction mixture was kept at room temperature for 3 h. After the solution was concentrated, complexes **III** and **IV** were isolated as diamagnetic crystalline substances colored in saturated red-violet. After filtration, the complexes were dried at room temperature in a vacuum of a roughing-down pump.

The yield of complex **III** was 0.489 g (70%).

For $C_{30}H_{47}N_3OS_4Sn$		
Anal. calcd., %	C 50.56	H, 6.65
Found, %	C, 50.68	H, 6.74

IR (ν, cm^{-1}): 1746 m, 1718 w, 1631 w, 1599 s, 1563 w, 1526 w, 1482 s, 1416 m, 1377 s, 1358 s, 1339 w, 1299 s, 1264 s, 1241 m, 1201 m, 1185 m, 1164 w, 1145 w, 1124 w, 1103 w, 1094 w, 1080 m, 1049 w, 1024 w, 996 w, 968 m, 928 m, 917 m, 877 s, 865 s, 830 s, 805 m, 774 m, 743 s, 671 w, 654 w, 645 w, 594 w, 559 m, 529 s, 477 m.

^{1}H NMR (C_6D_6, 20°C), δ, ppm: 7.56 (d, 1H, H_{AP}, J_{H-H} = 1.8 Hz); 7.09 (d, 1H, H_{AP}, J_{H-H} = 1.7 Hz); 2.33 (s, 12 H, Me); 1.88 (s, 9H, N(*t*-Bu)), 1.53 (s, 9H, (*t*-Bu)), 1.65 (s, 3H, –CH–); 2.78 (s, 6H, $-CH_2-$); 2.22 (s, 6H, $-CH_2-$). ^{13}C NMR (C_6D_6, 20°C), δ, ppm: 198.6 (C (TMTDS)); 138.1, 137.6 (C–(*t*-Bu)); 35.0 (C–O); 128.9 (C–N); 115.0–110.3 (C_{aryl}); 57.8 (N–C_{Ad}); 45.29 (CH_3 (TMTDS)); 37.8, 35.7 (CH_{2Ad}); 34.0 (CH_{Ad}); 32.2–30.7 (C_{quater}); 30.5 (CH_3(*t*-Bu)). ^{119}Sn NMR (C_6D_6, 20°C), δ, ppm: –656.5.

The yield of complex **IV** was 0.524 g (84%).

For $C_{24}H_{41}N_3OS_4Sn$		
Anal. calcd., %	C, 45.43	H, 6.51
Found, %	C, 45.65	H, 6.73

IR (ν, cm^{-1}): 1582 s, 1414 s, 1359 m, 1329 s, 1286 m, 1266 m, 1256 m, 1232 m, 1211 s, 1111 w, 1101 w, 1051 w, 1026 m, 994 s, 914 w, 870 s, 797 s, 775 w, 693 w, 656 m, 609 m, 534 w, 446 w.

^{1}H NMR (C_6D_6, 20°C), δ, ppm: 7.35 (d, 1H, H_{AP}, J_{H-H} = 2.2 Hz); 7.20 (d, 1H, H_{AP}, J_{H-H} = 2.2 Hz); 2.26 (s, 12 H, Me); 1.76 (s, 9H, N(*t*-Bu)), 1.43 (s, 9H, (*t*-Bu)), 1.19 (s, 9H, (*t*-Bu)).

^{119}Sn NMR (C_6D_6, 20°C), δ, ppm: –654.8.

Synthesis of complex V. A suspension of $Fe_2(CO)_9$ (0.28 g, 0.78 mmol) in toluene (10 mL) was added to a solution of stannylene **II** (0.280 g, 0.78 mmol) in the same solvent (10 mL). The reaction mixture was kept in the dark at 20°C for 2 days. Within this time the solution turned intensively brown. After the solution was concentrated to 10 mL, the yield of complex **V** as a yellow crystalline powder was 0.35 g (70%).

For $C_{28}H_{35}NO_5SnFe$		
Anal. calcd., %	C, 52.54	H, 5.51
Found, %	C, 52.71	H, 5.69

IR (ν, cm^{-1}): 2043 s, 1982 m, 1935 s, 1557 w, 1412 m, 1285 w, 1267 w, 1244 m, 1202 w, 1186 w, 1130 w, 1105 w, 1043 m, 972 m, 939 m, 939 m, 914 m, 872 m, 829 m, 804 m, 766 w, 750 m, 692 m, 665 m, 617 s, 549 w, 522 w.

^{1}H NMR (d_8-THF, 20°C), δ, ppm: 6.84 (d, 2H, J_{H-H} = 2.3 Hz, H_{AP}); 6.70 (d, 2H, J_{H-H} = 2.3 Hz, H_{AP}); 1.19 (s, 9H, *t*-Bu); 1.08 (s, 9H, *t*-Bu); 2.08 (s, 3H, –CH–); 2.05 (s, 6H, $-CH_2-$); 1.66 (s, 6H, $-CH_2-$). ^{13}C NMR (d_8-THF, 20°C), δ, ppm: 137.6, 134.3 (C–(*t*-Bu)); 125.9 (C–O); 124.6 (C–N); 120.8, 123.9 (C_{aryl}); 57.4 (N–C_{quater}); 34.4, 33.3 (C_{quater}); 31.6–29.6 (CH_3(*t*-Bu)); 211.1 (C=O).

IR spectra were recorded on an FSM-1201 FTIR spectrometer in Nujol in KBr cells. EPR spectra were detected on a Bruker EMX spectrometer. 2,2-Diphenyl-1-picrylhydrazyl (g = 2.0037) was used as a standard when determining the g factor. To determine exact parameters, the EPR spectrum was simulated using the WinEPR SimFonia program (Bruker).

Quantum chemical calculations were performed using the Gaussian 09 program package [43] by the

Table 1. Crystallographic data and structure refinement parameters for compounds **I**, **III**, and **IV**

Parameter	Value		
	I	**III**	**IV**
Empirical formula	$C_{48}H_{70}N_2O_2Sn_2$	$C_{30}H_{47}N_3OS_4Sn \cdot C_7H_8$	$C_{24}H_{41}N_3OS_4Sn \cdot CH_2Cl_2$
FW	944.44	804.77	719.45
Crystal system	Triclinic	Monoclinic	Monoclinic
Space group	$P\bar{1}$	*I*2/*a*	*I*2/*a*
T, K	100	298	100
a, Å	6.7263(4)	18.6353(4)	18.1573(16)
b, Å	12.6897(6)	12.9182(3)	17.3440(8)
c, Å	13.7217(7)	36.6481(9)	21.3163(10)
α, deg	99.1260(10)	90	90
β, deg	101.0710(10)	104.272(2)	91.8820(10)
γ, deg	101.3530(10)	90	90
V, Å^3	1103.20(10)	8550.2(4)	6709.3(7)
Z	1	8	8
ρ_{calc}, g/cm^3	1.422	1.250	1.425
μ, mm^{-1}	1.171	0.822	1.192
Crystal size, mm	0.52 × 0.22 × 0.18	0.76 × 0.15 × 0.11	0.40 × 0.14 × 0.14
Scan range over θ, deg	2.50–30.18	2.94–30.51	2.25–27.88
Number of measured/ Independent reflections	16202/6527	82190/13051	32826/7983
R_{int}	0.0151	0.0818	0.0402
Number of independent reflections with $I > 2\sigma(I)$	6286	7744	6721
Number of refined parameters/ restraints	250/0	452/160	396/21
R ($I > 2\sigma(I)$)	$R_1 = 0.0167$ $wR_2 = 0.0419$	$R_1 = 0.0474$ $wR_2 = 0.0917$	$R_1 = 0.0419$ $wR_2 = 0.0932$
R (for all data)	$R_1 = 0.0177$ $wR_2 = 0.0424$	$R_1 = 0.1017$ $wR_2 = 0.1066$	$R_1 = 0.0529$ $wR_2 = 0.1008$
S (F^2)	1.049	0.987	1.033
Residual electron density (min/max), e Å^{-3}	–0.27/0.72	–0.39/0.57	–0.78/1.18

density functional theory (DFT) with the B3LYP functional [44] and the standard def2svp basis set for all atoms.

The X-ray diffraction analyses of compounds **I**, **III**, and **IV** were carried out on Agilent Xcalibur E (**III**), Bruker Smart Apex (**IV**), and Bruker D8 Quest (**I**) diffractometers (ω scan mode, MoK_α radiation, λ = 0.71073 Å). Experimental sets of intensities were measured and integrated, absorption corrections were applied, and the structures were refined using the CrysAlis Pro [45], Smart, APEX2 [46], SADABS [47], SHELX [48] program packages. The structures were solved by a direct method and refined by full-matrix least squares for F^2_{hkl} in the anisotropic approximation for non-hydrogen atoms. The hydrogen atoms of complexes **I**, **III**, and **IV** were placed in geometrically calculated positions and refined isotropically with the fixed thermal parameters $U(H)_{iso} = 1.2U(C)_{eq}$ ($U(H)_{iso} = 1.5U(C)_{eq}$ for the methyl fragments).

The crystallographic data and parameters of X-ray diffraction experiments and structure refinement are presented in Table 1. The structures were deposited with the Cambridge Crystallographic Data Centre (CIF files CCDC nos. 1905419 (**I**), 1905420 (**III**), and 1905421 (**IV**)) and are available at ccdc.cam.ac.uk/structures.

RESULTS AND DISCUSSION

The tin(II) *o*-amidophenolate complex ^{Ad}APSn (**I**) was synthesized according to the procedure described earlier for the synthesis of $^{t\text{-Bu}}$APSn (**II**) [26]. The reaction of amine elimination between the corresponding *o*-aminophenol and tin(II) bis(trimethylsilyl)amide occurs with a high yield (~80%) in ether at room temperature (Scheme 1).

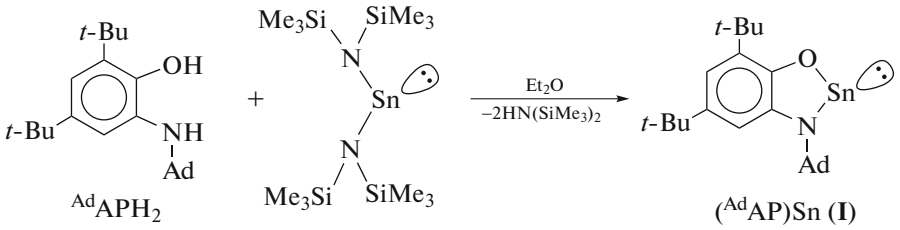

Scheme 1.

Stannylene **I** is a yellow crystalline product sensitive to air moisture and oxygen. The molecular and crystal structures of complex **I** were determined by X-ray diffraction analysis (Fig. 1). Selected bond lengths and angles are presented in Table 2. The Sn(1)–O(1) and Sn(1)–N(1) bond lengths (2.0533(8) and 2.2427(9) Å, respectively) are close to similar values for stannylene **II**. The O(1)–C(1) (1.349(2) Å) and N(1)–C(2) (1.463(2) Å) bond lengths and the C–C distances in the six-membered ring lying in a narrow range of 1.393(2)–1.416(2) Å and characteristic of aromatic systems unambiguously indicate [49, 50] the dianionic nature of the redox-active amidophenolate ligand. Stannylene **I** is dimerized in the crystalline state by strong intermolecular contacts Sn(1)–N(1*A*) 2.3153(9) Å (the sum of the van der Waals radii of tin and nitrogen is 3.8 Å [51]). The unoccupied *p* orbital at the tin atom acts as a strong Lewis acid toward the lone pair of the nitrogen atom of the adjacent molecule. This property predetermines the aggregation character of stannylenes [52–54]. In the dimer formed, the {SnNSnN} and {SnON} planes are close to orthogonal: the dihedral angle between them is 77.31(3)°. A similar character of the formation of dimeric molecules was observed for the previously published amidophenolate stannylenes containing the phenyl [22] and *tert*-butyl substituent [26] at the nitrogen atom. Remarkably, stannylene ^{Dipp}APSn [23] based on more sterically hindered 4,6-di-*tert*-butyl-*N*-(2,6-di-*iso*-propylphenyl)-*o*-aminophenol forms a dimer by intermolecular Sn···O contacts. It can be concluded that the character of dimerization of the complexes changes from Sn···O to Sn···N on going to less bulky substituents at the nitrogen atom.

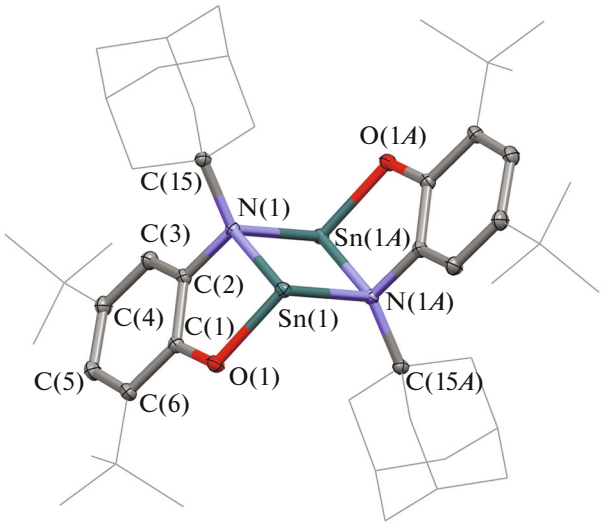

Fig. 1. Molecular structure of complex **I**. Thermal ellipsoids for the key atoms are presented with 50% probability. Hydrogen atoms are omitted for clarity.

Dimeric molecules of complex **I** form "infinite" chains due to the metallophilic interaction Sn···Sn (3.5360(2) Å) (Fig. 2), which is somewhat longer than that in sterically less hindered analog **II** (Sn···Sn 3.3523(2) Å [26]) and is comparable with the Sn···Sn distance in ^{Ph}ApSn 3.5480(2) Å [22]. The thorough study of the experimental electron density and the natural bond orbital (NBO) analysis for complex **II** showed the covalent character of this interaction [26]. As a result of the formation of chains of dimeric stannylene molecules, the adamantyl group deviates strongly from the {SnOCCN} plane (the deviation of the C(15) atom from the metallocycles plane is 1.12(2) Å). Thus, the nitrogen atom has the pyramidal configuration.

Presented above tin(II) *o*-amidophenolate complexes **I** and **II**, as well as other diimine and catecholate complexes [22, 25, 55] of Group 14 low-valence metals, can demonstrate multiple many-sided reactivity. The low-valence Sn(II) atom can be involved in the oxidative addition reactions to form the Sn(IV) derivatives (Scheme 2, route *a*). At the same time, the redox-active ligand can be involved in the redox interaction with the retention of the oxidation state of the

Table 2. Selected bond lengths (Å) and bond angles (deg) in complexes **I**, **III**, and **IV**

Bond	I	III	IV	Angle	I	III	IV
Sn(1)–N(1)	2.2427(9)	2.089(2)	2.092(3)	O(1)Sn(1)N(1)	80.13(3)	78.97(8)	79.25(9)
Sn(1)–O(1)	2.0533(8)	2.035(2)	2.034(2)	O(1)Sn(1)S(1)		103.91(5)	101.75(6)
C(1)–O(1)	1.349(2)	1.362(3)	1.359(4)	N(1)Sn(1)S(1)		100.88(6)	100.17(7)
C(2)–N(1)	1.463(2)	1.405(4)	1.404(4)	O(1)Sn(1)S(3)		159.69(6)	161.75(7)
C(1)–C(2)	1.414(2)	1.424(4)	1.428(4)	N(1)Sn(1)S(3)		108.74(6)	105.62(7)
C(2)–C(3)	1.398(2)	1.388(4)	1.400(4)	S(1)Sn(1)S(3)		93.24(3)	94.75(3)
C(3)–C(4)	1.393(2)	1.395(4)	1.393(5)	O(1)Sn(1)S(2)		86.75(6)	87.17(6)
C(4)–C(5)	1.398(2)	1.377(5)	1.394(4)	N(1)Sn(1)S(2)		160.80(6)	161.91(7)
C(5)–C(6)	1.399(2)	1.394(5)	1.402(4)	S(1)Sn(1)S(2)		70.02(3)	70.79(3)
C(6)–C(1)	1.416(2)	1.395(4)	1.403(4)	S(3)Sn(1)S(2)		89.02(3)	90.99(3)
Sn(1)–N(1*A*)	2.3153(9)			O(1)Sn(1)S(4)		90.09(5)	91.38(6)
Sn(1)–S(1)		2.5228(8)	2.5279(8)	N(1)Sn(1)S(4)		98.01(6)	100.74(7)
Sn(1)–S(2)		2.6110(9)	2.5818(9)	S(1)Sn(1)S(4)		158.29(3)	157.03(3)
Sn(1)–S(3)		2.5550(7)	2.5502(8)	S(3)Sn(1)S(4)		70.47(3)	70.50(3)
Sn(1)–S(4)		2.5708(7)	2.5930(8)	S(2)Sn(1)S(4)		94.74(3)	91.40(3)
S(1)–C		1.730(3)	1.735(3)	O(1)Sn(1)N(1*A*)	100.82(3)		
S(2)–C		1.707(3)	1.718(3)	N(1)Sn(1)N(1*A*)	81.24(3)		
S(3)–C		1.729(3)	1.732(3)	C(1)O(1)Sn(1)	115.96(6)		
S(4)–C		1.711(3)	1.726(3)	C(2)N(1)Sn(1)	106.26(6)		
				Sn(1)N(1)Sn(1*A*)	98.76(3)		

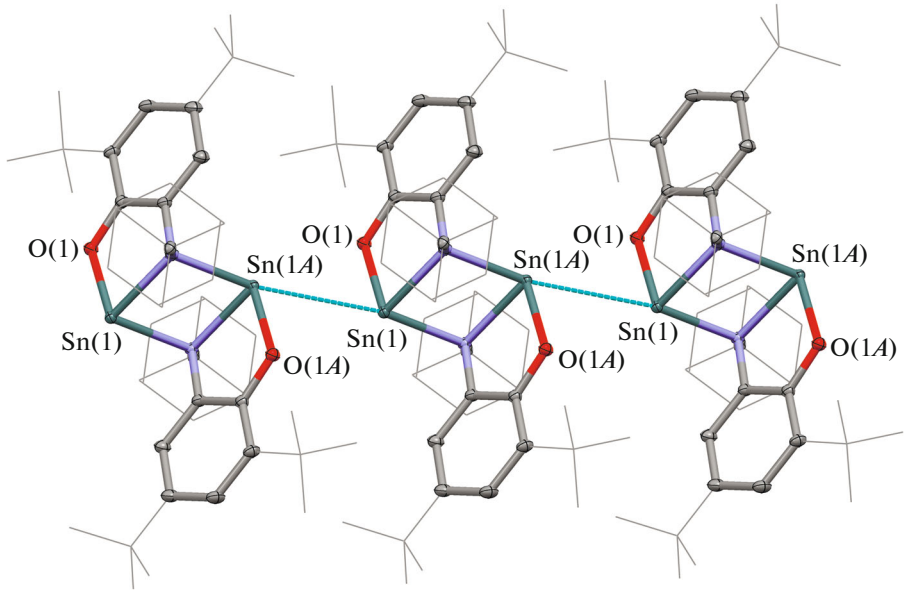

Fig. 2. Fragment of the crystal packing for complex **I**. Thermal ellipsoids for the key atoms are presented with 50% probability. Hydrogen atoms are omitted for clarity.

metal (Scheme 2, route *d*). Owing to the lone electron pair and unoccupied *p* orbital, stannylenes exhibit the Lewis amphotericity: they can act as both soft acids and soft bases (Scheme 2, routes *b* and *c*).

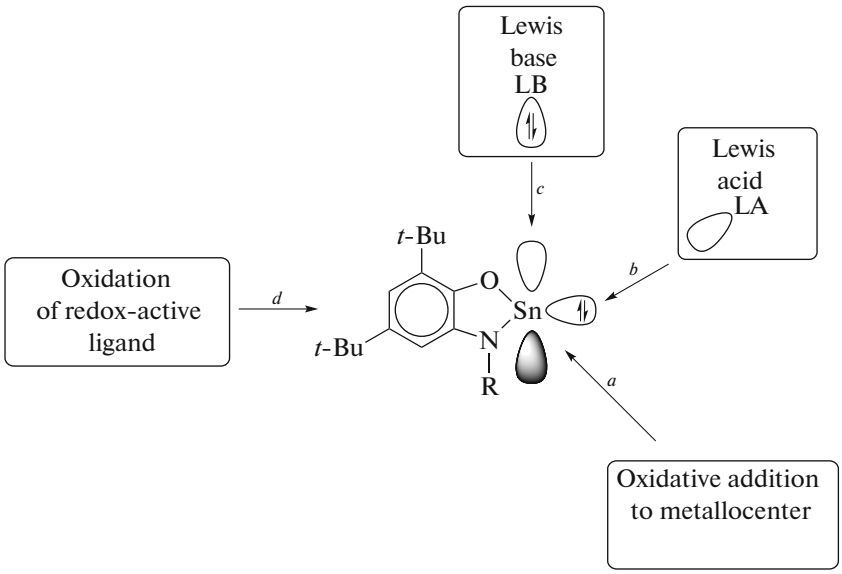

Scheme 2.

Disulfides are convenient reagents for studying various oxidative addition reactions [56–58]. For example, we have found that compounds **I** and **II** readily react with TMTDS taken in an equimolar amount to form violet crystalline diamagnetic products (^{Ad}AP)Sn(S_2R)$_2$ (**III**) and ($^{t\text{-Bu}}$AP)Sn(S_2R)$_2$ (**IV**) (Scheme 3). The reaction completes within several hours at room temperature. Under these reaction conditions, the homolytic dissociation of the S–S bond in disulfide should not be expected, since the thermal dissociation of TMTDS occurs at T = 130–150°C [59]. Therefore, the process studied is accompanied by the insertion of the low-valence tin atom at the S–S bond followed by the formation of new hexacoordinated tin(IV) dithiocarbamate complexes.

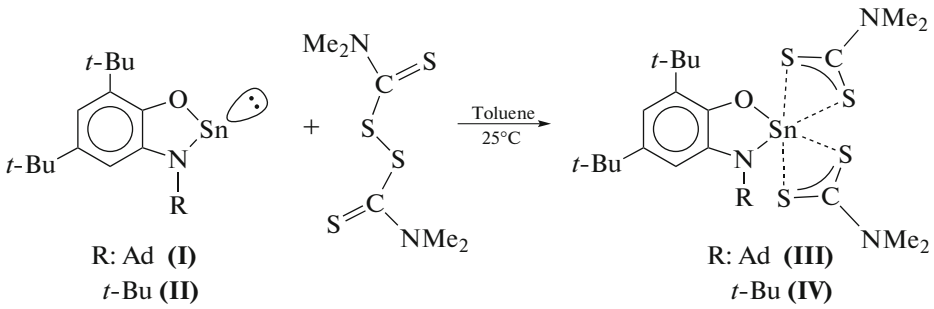

Scheme 3.

The molecular and crystal structures of complexes **III** and **IV** (Fig. 3) were determined by X-ray diffraction analysis. The crystals suitable for X-ray diffraction analysis were obtained from toluene (**III**) and an *n*-hexane–CH_2Cl_2 mixture (**IV**). The independent region of the crystalline cells of compounds **III** and **IV** contains one solvate toluene molecule (**III**) and dichloromethane molecule (**IV**) along with the molecules of the complexes. The geometric characteristics of complexes **III** and **IV** are close to each other (Table 2) and, hence, below we discuss only the molecular structure of complex **IV**.

The coordination environment of the metal atom in complex **IV** is a distorted octahedron. The Sn(1)–O(1) (2.034(2) Å) and Sn(1)–N(1) (2.092(3) Å) bond lengths in compound **IV** are less than the sum of the covalent radii of the corresponding elements (2.09 Å for Sn–O, 2.1 Å for Sn–N [51]) and are close to those in tin(IV) *o*-amidophenolates [22, 42]. These bonds are substantially shorter than those observed in the

initial stannylene **I**, which agrees with a change in the oxidation state of the central tin(II) atom to tin(IV).

The C(1)–O(1) (1.359(4) Å) and C(2)–N(1) (1.404(4) Å) distances lie in a range characteristic of the dianionic form of the *o*-iminoquinone ligand [49, 50]. The C–C bonds in the six-membered ring are close to typically aromatic values of ~1.40 Å. The obtained metric parameters indicate the dianionic state of the redox-active ligand. Each dithiocarbamate fragment chelates the metallocenter via the bidentate mode to form four-membered rings $\{CS_2Sn\}$. The SSnS angles (70.50(3)°, 70.79(3)°) in the rings are close to 70°. The Sn–S bond lengths range from 2.5279(8) to 2.5930(8) Å. The C–S distances in the dithiocarbamate fragments are close (1.718(3)–1.735(3) Å, average C–S is 1.728(6) Å) and indicate a significant charge delocalization in the considered fragment [60].

The ability of stannylene **I** to present the unoccupied *p* for the donor–acceptor interaction was clearly demonstrated by the formation of dimeric molecules in the corresponding crystals. There is large literature data body on the complex formation of the low-valence tin derivatives with transition metals by the involvement of the lone electron pair of the metallene into the interaction [61]. It should be mentioned that stannylenes act as Lewis bases in the case. The reaction of complex **I** with $Fe_2(CO)_9$ in a toluene solution completes at room temperature within 2 days and gives adduct **V** as a yellow-brown finely crystalline powder (Scheme 4).

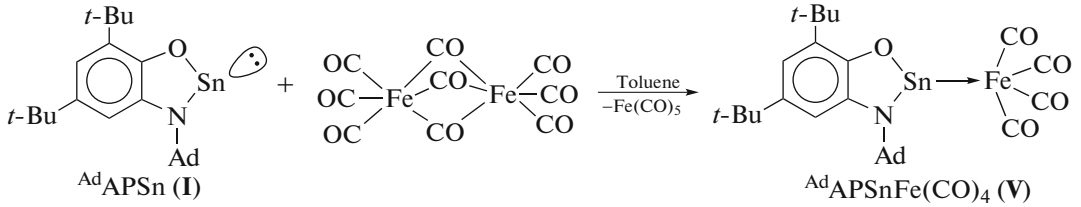

Scheme 4.

The product formed was identified using ^1H and ^{13}C NMR spectroscopy and IR spectroscopy data. The ^1H NMR spectrum of compound **V** exhibits an insignificant shift of all signals compared to the spectrum of the initial stannylene **I**. The ^{13}C NMR spectrum is characterized by the appearance of a new signal at δ_C 210.7 ppm belonging to the carbonyl groups bound to the iron atom. The vibrations of the carbonyl CO bonds in complex **V** appear in the IR spectrum as strong absorption bands in a range of 1980–2043 cm^{-1}.

As shown above, stannylenes **I** and **II** react with TMTDS to form the tin(IV) derivatives (Scheme 3). During this reaction, the redox-active ligand does not change its oxidation state. The introduction of soft one-electron oxidants into the reactions with compounds **I** and **II** makes it possible to transfer the reaction center from the metal to ligand retaining the oxidation state of the metal.

We studied the reactions of the synthesized tin(II) *o*-amidophenolates with such oxidants as mercury salts $HgHal_2$ (Hal = Cl, Br, I) and stable 2-ethoxy-3,6-di-*tert*-butyl-2-ethoxyphenoxyl radical (hereinafter phenoxyl) [39].

It is known that the paramagnetic derivatives of Group 14 elements based on the radical redox-active ligands are very labile [22, 55, 62, 63]. At the moment, only two works are known where they were isolated in the individual state [33, 34]. We succeeded to detect the signals corresponding to the paramagnetic tin(II) derivatives of the general formula (^{R}ImSQ)SnOR in the EPR spectra during the reactions of compounds **I** and **II** with phenoxyl (^{R}ImSQ is the radical-anionic form of the ligand). Under the EPR experimental conditions, upon the oxidation of complex **II** by phenoxyl, the reaction mixture turns intensively green and a well resolved signal is observed in the spectrum (Fig. 4a) indicating the formation of the corresponding tin(II) mono-*o*-iminosemiquinolate derivative ($^{t\text{-Bu}}$ImSQ)-SnOR (**VI**). The spectrum of the obtained radical-anionic complex **VI** is a triplet (1 : 1 : 1) of doublets (1 : 1). The hyperfine structure of the spectrum is due to the hyperfine coupling (HFC) of the lone electron with two nonequivalent magnetic nuclei of the ^1H hydrogen atom (99.98%, $I = 1/2$, $\mu_N = 2.7928$) [64] and ^{14}N nitrogen atom (99.63%, $I = 1$, $\mu_N = 0.4037$) [64]. In addition, the satellite splitting on the ^{117}Sn (7.68%, $I = 1/2$, $\mu_N = 1.000$) and ^{119}Sn (8.58%, $I = 1/2$, $\mu_N = 1.046$) [64] tin magnetic isotopes is observed. The parameters of the EPR spectrum (Table 3) observed in the course of the reaction of complex **II** with phenoxyl, namely, high HFC constants $a_i(^{119}Sn) = 145.0$ Oe, $a_i(^{119}Sn) = 138.6$ Oe, differ substantially from those obtained previously for tin(IV) *o*-iminosemiquinolates [65, 66]. The latter are characterized by the lower HFC constants $a_i(^{117,\ 119}Sn)$ (20–50 Oe). On the contrary, the divalent tin compounds are usually characterized by the high HFC constants ($a_i^{117,\ 119}Sn \geq 90$ Oe) [22, 55, 67, 68].

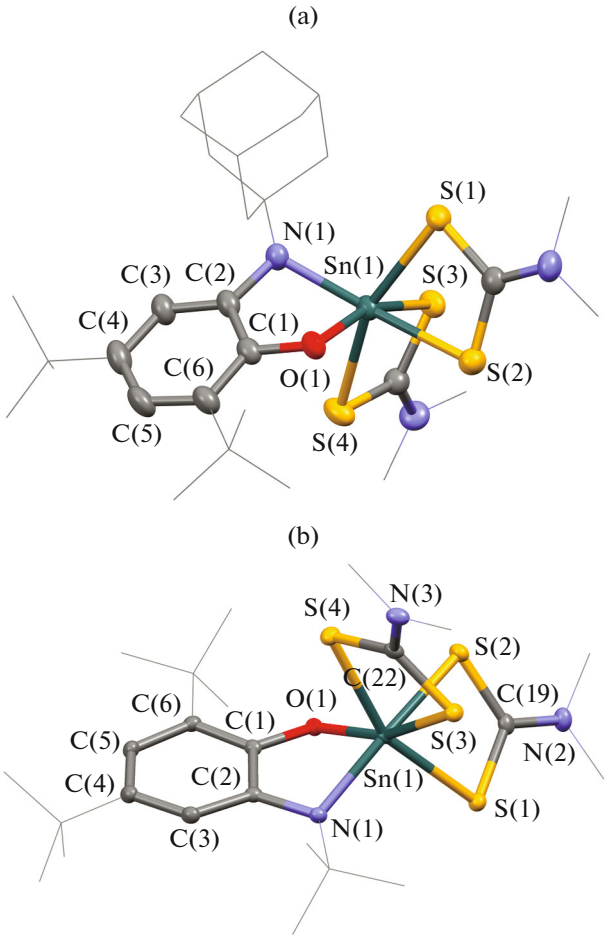

Fig. 3. Molecular structures of the complexes: (a) (^{Ad}AP)Sn(S_2R)$_2$ (**III**) and (b) ($^{t\text{-}Bu}$AP)Sn(S_2R)$_2$ (**IV**). Thermal ellipsoids for the key atoms are presented with 50% probability. Hydrogen atoms are omitted for clarity.

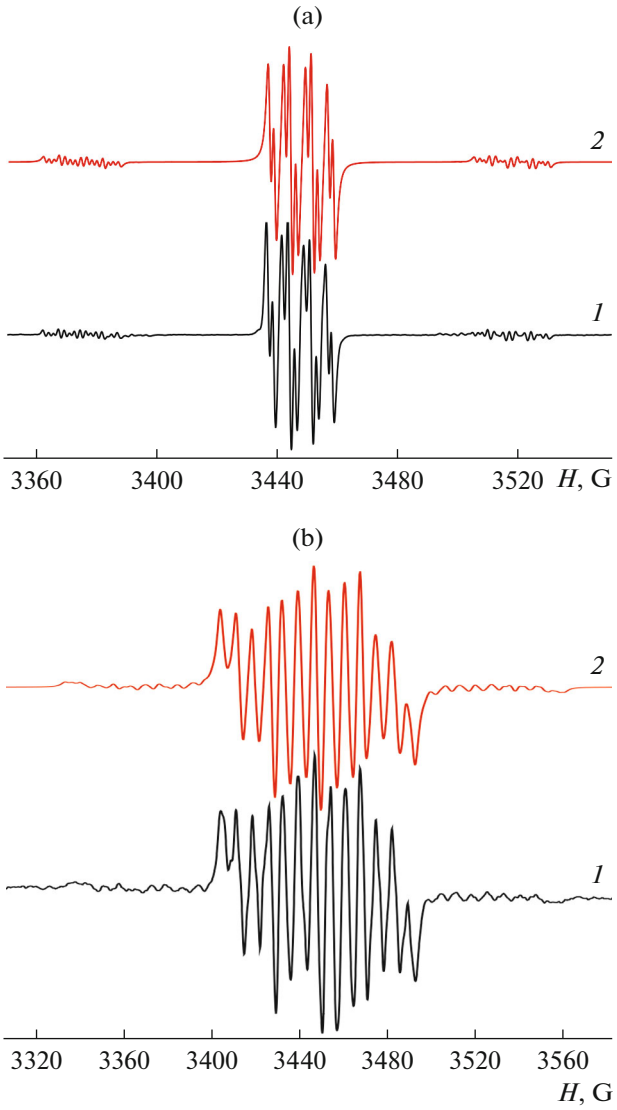

Fig. 4. Isotropic EPR spectra of complexes (a) **VI** and (b) **IX** in THF: (*1*) experimental and (*2*) simulated at 298 K.

The differences observed in values of the HFC constants with the magnetic isotopes of the metal in the high- and low-valence states are typical of both tin and other elements [69, 70]. Based on the EPR spectroscopy data, we can unambiguously conclude that the reaction mixture contains species consisting of the *o*-iminosemiquinone ligand and the metal in the low oxidation state.

The intensive green color and the corresponding EPR spectrum typical of *o*-iminosemiquinone complex **VI** are retained for ~1.5 h. The storage of the reaction mixture at room temperature for 2 h results in an

Table 3. Parameters of the isotropic EPR spectra (Oe) for complexes **VI–IX**

Complex	g_i	$a_i(^1H)$	$a_i(^1H)$	$a_i(^{14}N)$	$a_i(^{119}Sn)$	$a_i(^{117}Sn)$	a_i(Hal)
VI	2.0008	2.0	5.1	7.2	145.0	138.6	
VII	2.0003	1.6	5.2	7.0	145.8	139.0	
VIII	2.0003	1.2	5.5	7.3	138.0	132.1	4.3 (^{35}Cl) 3.5 (^{37}Cl)
IX	2.0013	1.2	5.4	7.2	138.4	132.3	17.0 (^{79}Br) 20.5 (^{81}Br)

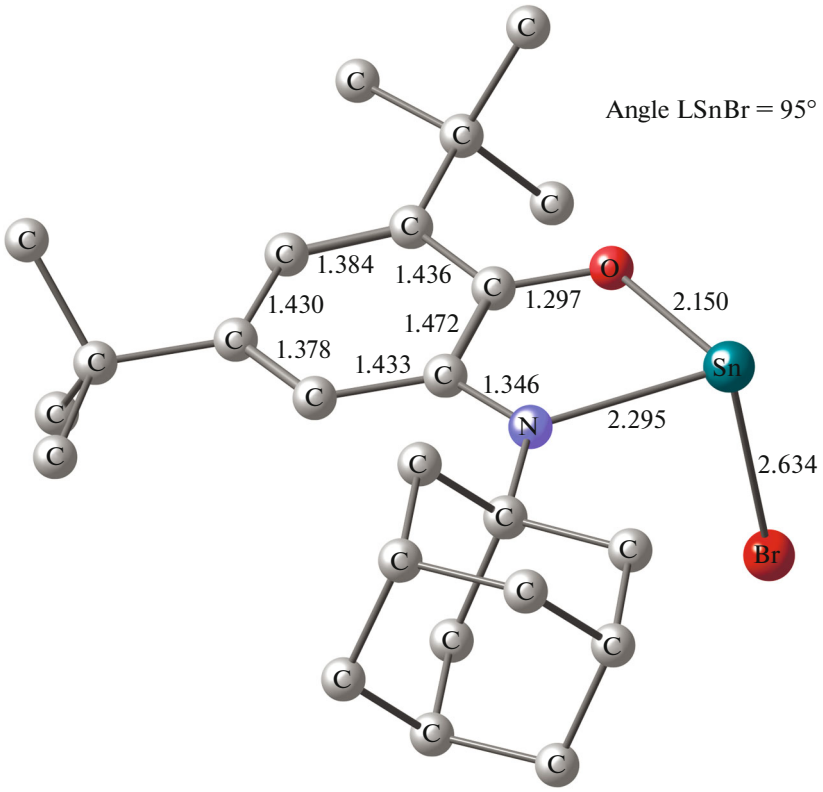

Fig. 5. Optimized geometry of complex **IX** (DFT B3LYP/def2svp). Hydrogen atoms are omitted for clarity. Bond lengths are presented in Å.

intensive yellow coloration and the complete disappearance of the signal from the EPR spectrum. A similar behavior is demonstrated by stannylene **I**, whose reaction with phenoxyl affords the paramagnetic derivative (^{Ad}ImSQ)SnOR (**VII**). The parameters of the EPR spectra of paramagnetic stannylenes **VI**–**IX** are presented in Table 3.

It is important that the detected paramagnetic stannylenes **VI** and **VII** are substantially more stable than their *N*-aryl-substituted analogs. Similar paramagnetic species (^{Dipp}ImSQ)SnOR were observed in solutions only at decreased temperatures (–18°C) [22]. In addition, we succeeded to detect the EPR spectra corresponding to halogen-containing radical stannylenes (^{Ad}ImSQ)SnCl (**VIII**) and (^{Ad}ImSQ)SnBr (**IX**) during the reaction of compound **I** with mercury(II) halides (Table 3). The EPR spectrum of complex **IX** is presented in Fig. 4b. We failed to detect the products with the iodide ion at the metal atom and with the *N*-*tert*-butyl substituent in the redox-active ligand because of their fast transformation even at low temperatures.

The hyperfine structure of the spectrum of complex **IX** is due to the interaction of the lone electron with two nonequivalent magnetic nuclei of the ^{1}H hydrogen atom, ^{14}N nitrogen atom, and magnetic ^{79,81}Br bromide isotopes. The satellite splitting on the magnetic ^{117,119}Sn isotopes is also observed. The high HFC constants with the magnetic isotopes of the halogen substituents indicate that the $\sigma(\sigma^*)$ orbitals of Sn–Hal appreciably contribute to the π molecular orbital occupied by the lone electron.

The most probable geometry of the formed intermediate stannylene **IX** was determined by quantum chemical modeling (DFT B3LYP/def2svp) (Fig. 5). The tin atom in compound **IX** has the trigonal pyramidal coordination mode. The halogen atom is almost orthogonal to the plane of the redox-active ligand (the LSnBr angle is 95°), which provides the efficient overlapping of the orbital of the lone electron and the $\sigma(\sigma^*)$ orbital of Sn–Hal.

Based on the results obtained on the oxidation of the considered stannylenes, we may conclude that the formed nonsymmetrical tin(II) derivatives of the general formula (^{R}ImSQ)SnX are instable in solutions. After the end of the reactions of compound **I**, only earlier known tin(IV) bis-*o*-amidophenolates were isolated from the reaction mixtures [42]. The following mechanism can be proposed for the oxidation of complexes **I** and **II** on the basis of the data of EPR spectroscopy and reaction products (Scheme 5):

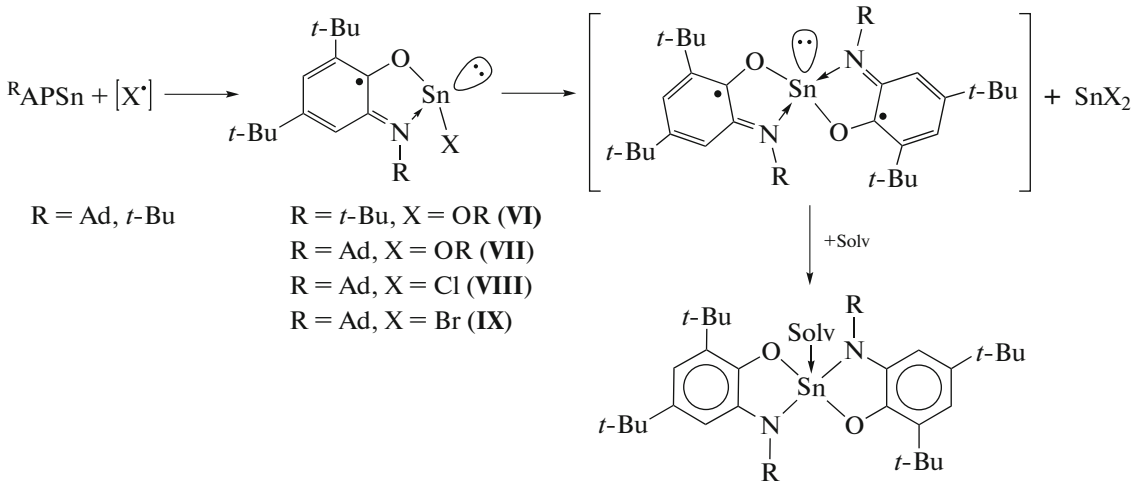

R = Ad, *t*-Bu

R = *t*-Bu, X = OR (**VI**)
R = Ad, X = OR (**VII**)
R = Ad, X = Cl (**VIII**)
R = Ad, X = Br (**IX**)

Scheme 5.

In the first step, the one-electron oxidation of the initial stannylene occurs to form the paramagnetic tin(II) derivative with the general formula (^{R}ImSQ)SnX. Complexes of this type are unstable and symmetrized to form biradical products of the (^{R}ImSQ)$_2$Sn^{II} and SnX_2 types. In the last step, the (^{R}ImSQ)$_2$Sn^{II} derivatives undergo the intramolecular redox process, which consists of the oxidation of the metallocenter to the tetravalent state and the transition of the redox-active ligands to the dianionic form. The possibility of this redox-isomeric transformation was described earlier [42].

Thus, the redox-active ligands affect the reactivity of the metallocenter and also are actively involved themselves in redox reactions with diverse substrates without losing bonding with the complexing agent.

The new complex of low-valence tin (^{Ad}AP)Sn was synthesized in this study. The saturation of the coordination sphere of the metal in the crystalline state was shown to be achieved due to intermolecular donor–acceptor interactions. Similar compounds can react with Lewis acid and have a dual nature in redox transformations: the redox-active ligand is responsible for the reactions with one-electron oxidants, whereas the divalent metal ion is responsible for the reactions with two-electron oxidants.

ACKNOWLEDGMENTS

The X-ray diffraction studies were carried out in the framework of the state task using the scientific equipment of the Center for Collective Use “Analytical Center of the Razuvaev Institute of Organometallic Chemistry of the Russian Academy of Sciences.”

FUNDING

This work was supported by Russian Science Foundation, project no. 17-13-01428.

CONFLICT OF INTEREST

The authors declare that they have no conflicts of interest.

REFERENCES

1. Abakumov, G.A., Piskunov, A.V., Cherkasov, V.K., et al., *Russ. Chem. Rev.*, 2018, vol. 87, p. 393.
2. Luca, O.R. and Crabtree, R.H., *Chem. Soc. Rev.*, 2013, vol. 42, p. 1440.
3. Broere, D.L.J., Plessius, R., and van der Vlugt, J.I., *Chem. Soc. Rev.*, 2015, vol. 44, p. 6886.
4. Kaim, W. and Paretzki, A., *Coord. Chem. Rev.*, 2017, vol. 344, p. 345.
5. Jacquet, J., Murr, M.D., and Fensterbank, L., *ChemCatChem*, 2016, vol. 8, p. 3310.
6. Kaim, W., *Inorg. Chem.*, 2011, vol. 50, p. 9752.
7. Lyaskovskyy, V. and de Bruin, B., *ACS Catal.*, 2012, vol. 2, p. 270.
8. Tezgerevska, T., Alley, K.G., and Boskovic, C., *Coord. Chem. Rev.*, 2014, vol. 268, p. 23.
9. Schulz, S., *Chem.-Eur. J.*, 2010, vol. 16, p. 6416.
10. Hadlington, T.J., Driess, M., and Jones, C., *Chem. Soc. Rev.*, 2018, vol. 47, p. 4176.
11. Li, Z., Thiery, G., Lichtenthaler, M.R., Guillot, R., et al., *Adv. Synth. Catal.*, 2018, vol. 360, p. 544.
12. Yadav, S., Saha, S., and Sen, S.S., *ChemCatChem*, 2016, vol. 8, p. 486.
13. Kazarina, O.V., Gourlaouen, C., Karmazin, L., et al., *Dalton Trans.*, 2018, vol. 47, p. 13800.
14. Benedek, Z. and Szilvasi, T., *Organometallics*, 2017, vol. 36, p. 1591.
15. Kühl, O., *Coord. Chem. Rev.*, 2004, vol. 248, p. 411.
16. Tokitoh, N. and Okazaki, R., *Coord. Chem. Rev.*, 2000, vol. 210, p. 251.
17. Asay, M., Jones, C., and Driess, M., *Chem. Rev.*, 2011, vol. 111, p. 354.
18. Mizuhata, Y., Sasamori, T., and Tokitoh, N., *Chem. Rev.*, 2009, vol. 109, p. 3479.

19. Lee, V.Y. and Sekiguchi, A., *Organometallic Compounds of Low-Coordinate Si, Ge, Sn and Pb: From Phantom Species to Stable Compounds*, Chichester: Wiley, 2010.
20. Mandal, S.K. and Roesky, H.W., *Acc. Chem. Res.*, 2012, vol. 45, p. 298.
21. Abakumov, G.A., Cherkasov, V.K., Piskunov, A.V., et al., *Izv. Akad. Nauk. Ser. Khim.*, 2006, p. 1103.
22. Chegerev, M.G., Piskunov, A.V., Maleeva, A.V., et al., *Eur. J. Inorg. Chem.*, 2016, p. 3813.
23. Piskunov, A.V., Aivaz'yan, I.A., Fukin, G.K., et al., *Inorg. Chem. Commun.*, 2006, vol. 9, p. 612.
24. Tsys, K.V., Chegerev, M.G., Fukin, G.K., and Piskunov, A.V., *Mendeleev Commun.*, 2018, vol. 28, p. 527.
25. Tsys, K.V., Chegerev, M.G., Pashanova, K.I., et al., *Inorg. Chim. Acta*, 2019, vol. 490, p. 220.
26. Chegerev, M.G., Piskunov, A.V., Tsys, K.V., et al., *Eur. J. Inorg. Chem.*, 2019, p. 875.
27. Chegerev, M.G. and Piskunov, A.V., *Russ. J. Coord. Chem.*, 2018, vol. 44, p. 258. https://doi.org/10.1134/S1070328418040036
28. Zabula, A.V. and Hahn, F.E., *Eur. J. Inorg. Chem.*, 2008, p. 5165.
29. Gans-Eichler, T., Gudat, D., Nattingen, K., and Nieger, M., *Chem.-Eur. J.*, 2006, vol. 12, p. 1162.
30. Leites, L.A., Bukalov, S.S., Aysin, R.R., et al., *Organometallics*, 2015, vol. 34, p. 2278.
31. Fedushkin, I.L., Skatova, A.A., Chudakova, V.A., et al., *Organometallics*, 2004, vol. 23, p. 3714.
32. Druzhkov, N.O., Kazakov, G.G., Shavyrin, A.S., et al., *Inorg. Chem. Commun.*, 2018, vol. 90, p. 92.
33. Fedushkin, I.L., Khvoinova, N.M., Baurin, A.Y., et al., *Inorg. Chem.*, 2004, vol. 43, p. 7807.
34. Janes, T., Zatsepin, P., and Song, D.T., *Chem. Commun.*, 2017, vol. 53, p. 3090.
35. Fedushkin, I.L., Sokolov, V.G., Piskunov, A.V., et al., *Chem. Commun.*, 2014, vol. 50, p. 10108.
36. Gordon, A. and Ford, R., *The Chemist's Companion: A Handbook of Practical Data, Techniques, and References*, New York: Wiley, 1972.
37. Abakumov, G.A., Cherkasov, V.K., and Nevodchikov, V.I., *Tetrahedron Lett.*, 2005, vol. 46, p. 4095.
38. Brauer, G., *Handbuch der Praparativen Anorganischen Chemie*, Print book, German, 1981.
39. Harris, D.H. and Lappert, M.F., *Chem. Commun.*, 1974, p. 895.
40. Matson, E.M., Opperwall, S.R., Fanwick, P.E., and Bart, S.C., *Inorg. Chem.*, 2013, vol. 52, p. 7295.
41. Shadyro, O.I., Sorokin, V.L., Ksendzova, G.A., et al., *Pharm. Chem. J.*, 2012, vol. 46, p. 27.
42. Chegerev, M.G., Piskunov, A.V., and Starikova, A.A., *Eur. J. Inorg. Chem.*, 2018, p. 1087.
43. Frisch, M.J., Trucks, G.W., Schlegel, H.B., et al., *Gaussian 09. Revision D.01*, Wallingford: Gaussian, Inc., 2013.
44. Becke, A.D., *J. Chem. Phys.*, 1993, vol. 98, p. 5648.
45. *Agilent. CrysAlis Pro*, Yarnton (Oxfordshire): Agilent Technologies Ltd., 2014.
46. *Smart. APEX2*, Madison: Bruker AXS Inc., 2014.
47. Krause, L., Herbst-Irmer, R., Sheldrick, G.M., and Stalke, D., *J. Appl. Crystallogr.*, 2015, vol. 48, p. 3.
48. Sheldrick, G.M., *Acta Crystallogr., Sect. C: Struct. Chem.*, 2015, vol. 71, p. 3.
49. Brown, S.N., *Inorg. Chem.*, 2012, vol. 51, p. 1251.
50. Poddel'sky, A.I., Cherkasov, V.K., and Abakumov, G.A., *Coord. Chem. Rev.*, 2009, vol. 253, p. 291.
51. Batsanov, S.S., *Zh. Neorg. Khim.*, 1991, vol. 36, p. 3015.
52. Mansell, S.M., Russell, C.A., and Wass, D.F., *Inorg. Chem.*, 2008, vol. 47, p. 11367.
53. Aysin, R.R., Leites, L.A., Bukalov, S.S., et al., *Inorg. Chem.*, 2016, vol. 55, p. 4698.
54. Zabula, A.V., Rogachev, A.Y., and West, R., *Chem.-Eur. J.*, 2014, vol. 20, p. 16652.
55. Piskunov, A.V., Aivaz'yan, I.A., Cherkasov, V.K., and Abakumov, G.A., *J. Organomet. Chem.*, 2006, vol. 691, p. 1531.
56. Broere, D.L.J., Metz, L.L., de Bruin, B., et al., *Angew. Chem., Int. Ed. Engl.*, 2015, vol. 54, p. 1516.
57. Fedushkin, I.L., Maslova, O.V., Hummert, M., and Schumann, H., *Inorg. Chem.*, 2010, vol. 49, p. 2901.
58. Fedushkin, I.L., Nikipelov, A.S., Skatova, A.A., et al., *Eur. J. Inorg. Chem.*, 2009, p. 3742.
59. Steudel, R., Steudel, Y., Mak, A.M., and Wong, M.W., *Org. Chem.*, 2006, vol. 71, p. 9302.
60. Bouška, M., Novák, M., Dostál, L., et al., *Eur. J. Inorg. Chem.*, 2014, p. 310.
61. Baumgartner, J. and Marschner, C., Rev. *Inorg. Chem.*, 2014, vol. 34, p. 119.
62. Tumanskii, B., Pine, P., Apeloig, Y., et al., *J. Am. Chem. Soc.*, 2004, vol. 126, p. 7786.
63. Tumanskii, B., Pine, P., Apeloig, Y., et al., *J. Am. Chem. Soc.*, 2005, vol. 127, p. 8248.
64. Emsley, J., *The Elements*, London: Clarendon, 1991.
65. Piskunov, A.V., Meshcheryakova, I.N., Baranov, E.V., et al., *Izv. Akad. Nauk. Ser. Khim.* 2010, p. 354.
66. Piskunov, A.V., Chegerev, M.G., Vaganova, L.B., and Fukin, G.K., *Russ. J. Coord. Chem.*, 2015, vol. 41, p. 428. https://doi.org/10.1134/S1070328415070076
67. Abakumov, G.A., Cherkasov, V.K., Piskunov, A.V., and Druzhkov, N.O., *Dokl. Akad. Nauk*, 2004, vol. 399, p. 353.
68. Chegerev, M.G., Piskunov, A.V., and Starikova, A.A., *Zh. Obshch. Khim.,* 2017, vol. 76, p. 1841.
69. Abakumov, G.A., Nevodchikov V.I., Cherkasov, V.K., and Razuvaev, G.A., *Dokl. Akad. Nauk SSSR*, 1978, vol. 242, p. 609.
70. Klimov, E.S., Abakumov, G.A., Gladyshev, E.N., et al., *Dokl. Akad. Nauk SSSR*, 1974, vol. 218, p. 844.

Translated by E. Yablonskaya